

AD-A051 178

INDIANA UNIV BLOOMINGTON DEPT OF CHEMISTRY
ATOMIC EMISSION SPECTROMETRY OF TRACE METALS USING A NEW KIND O--ETC(U)
FEB 78 A T ZANDER, G M HIEFTJE

F/G 11/6

N00014-76-C-0838

UNCLASSIFIED

11

NL

| QF |
AD
A051178



END
DATE
FILMED

4-78

DDC

UNCLASSIFIED

SECURITY CLASSIFICATION OF THIS PAGE (When Data Entered)

12

AD A 051178

REPORT DOCUMENTATION PAGE		READ INSTRUCTIONS BEFORE COMPLETING FORM
1. REPORT NUMBER ELEVEN	2. GOVT ACCESSION NO.	3. RECIPIENT'S CATALOG NUMBER
6. TITLE (and Subtitle) ATOMIC EMISSION SPECTROMETRY OF TRACE METALS USING A NEW KIND OF MICROWAVE-INDUCED HELIUM PLASMA AT ATMOSPHERIC PRESSURE		5. TYPE OF REPORT & PERIOD COVERED
7. AUTHOR(s) Andrew T. Zander and Gary M. Hieftje		6. PERFORMING ORG. REPORT NUMBER 14-11
9. PERFORMING ORGANIZATION NAME AND ADDRESS Department of Chemistry Indiana University Bloomington, Indiana 47401		8. CONTRACT OR GRANT NUMBER(s) N00014 NSF-CHE76-10896
11. CONTROLLING OFFICE NAME AND ADDRESS Office of Naval Research Washington, D.C.		10. PROGRAM ELEMENT, PROJECT, TASK AREA & WORK UNIT NUMBERS NR 051-622
14. MONITORING AGENCY NAME & ADDRESS (if different from Controlling Office)		12. REPORT DATE 12 February 1978
		13. NUMBER OF PAGES 25 (12) 124P
		15. SECURITY CLASS. (of this report) UNCLASSIFIED
16. DISTRIBUTION STATEMENT (of this Report) Approved for public release; distribution unlimited		15a. DECLASSIFICATION/DOWNGRADING SCHEDULE
17. DISTRIBUTION STATEMENT (of the abstract entered in Block 20, if different from Report)		DDC MAR 14 1978
18. SUPPLEMENTARY NOTES Prepared for publication in ANALYTICAL CHEMISTRY		F
19. KEY WORDS (Continue on reverse side if necessary and identify by block number)		
20. ABSTRACT (Continue on reverse side if necessary and identify by block number) A recently described resonant cavity for generating microwave-induced helium plasmas (MIPs) at atmospheric pressure has been evaluated for use in the emission spectrometric determination of metallic elements, and has been found to offer several advantages over alternative designs. The new cavity allows self-ignition of an atmospheric pressure helium MIP. In addition, the plasma which is formed exhibits significantly improved operational stability and is considerably less susceptible to injected aerosol samples. The helium MIP was (continued)		

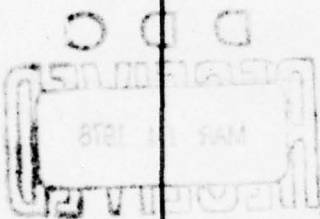
AD No. DDC FILE COPY

176 685 JOB

UNCLASSIFIED

SECURITY CLASSIFICATION OF THIS PAGE(When Data Entered)

used in conjunction with a single-shot microarc sample atomizer. With this combination, analytical calibration curves for Zn, Pb, Mn, Mg, Cu, Ca, and Na are linear over 2 to 5 orders of magnitude of concentration; also, detection limits for these elements are equal to or better than those obtainable with other MIPs. As with most MIPs, the ionization of easily ionized elements must either be overcome using ionization suppressants or exploited through use of ion emission lines. Interference from refractory elements is lower than exhibited by most MIPs.



UNCLASSIFIED

SECURITY CLASSIFICATION OF THIS PAGE(When Data Entered)

ATOMIC EMISSION SPECTROMETRY OF TRACE METALS USING A NEW KIND OF
MICROWAVE-INDUCED HELIUM PLASMA AT ATMOSPHERIC PRESSURE

Andrew T. Zander^a and Gary M. Hieftje^{*}

Department of Chemistry
Indiana University
Bloomington, Indiana 47401

a Present Address Department of Chemistry, Cleveland State
University, Cleveland, Ohio 44115

INTRODUCTION
 ~~~~~

A new design of resonant cavity for the generation of 2450 MHz microwave-induced plasmas (MIPs) has been recently described (1). The cavity has a minimal internal volume so that energy density in the plasma chamber at a given input power level is high enough to allow self-ignition of a helium plasma at atmospheric pressure. Subsequent communications (2,3) concerning this cavity have dealt with the theory of its design, probable excitation mechanisms in plasmas formed within it, and its use as a halogen and nonmetallic element detector for gas chromatography.

The high excitation capability and greatly improved stability of atmospheric pressure helium plasmas formed in this cavity suggest its further application as an excitation source for metallic elements in aqueous sample solutions. Accordingly, we have constructed, with minor modification, a version of the cavity described by Beenakker (1-3) with a microarc atomization unit (4). The microarc atomizer has also been modified, to enable its operation in helium. The operational characteristics of the resulting microarc/MIP excitation source and its usefulness for the atomic emission detection of several metallic elements have been studied.

|                                                      |                                                   |
|------------------------------------------------------|---------------------------------------------------|
| ACCESSION for                                        |                                                   |
| NTIS                                                 | White Section <input checked="" type="checkbox"/> |
| DOC                                                  | Buff Section <input type="checkbox"/>             |
| EXEMPTED FROM DISSEMINATION <input type="checkbox"/> |                                                   |
| 4 S I G N I F I C A N T                              |                                                   |
| BY                                                   |                                                   |
| DISTRIBUTION/AVAILABILITY CODES                      |                                                   |
| SPECIAL                                              |                                                   |
| A                                                    |                                                   |

### EXPERIMENTAL

A modified microwave cavity was machined from a single piece of 5 inch (12.7 cm) diameter Cu cylindrical bar stock. The finished cavity, shown in Figure 1, is about 1.5 inches (3.8 cm) thick and weighs about 5 pounds (2.3 kg). The cavity is essentially a fixed well 10 mm deep with a removable lid held in place by 12 bolts to ensure good electrical contact. The thickness of the cavity walls and bottom were increased over those of the previous design (1) for easier construction and mechanical stability. Also, the microwave power input connector was belted directly to the cavity, without further modification (1). The coupling loop (1), constructed of 1 mm diameter Cu wire, extended into the cavity 10 mm and is silver-soldered to the cavity bottom. A 7 mm hole is formed in the center of the well and lid to allow insertion of the quartz plasma chamber into the cavity. Because the introduction of dielectric material such as the quartz chamber into the cavity lowers the cavity's resonant frequency (1,5), the internal diameter of the cavity must be less than the resonant  $3/4$ -wave distance calculated to be 93.7mm at 2450 MHz. Thus, the cavity was constructed with an internal diameter of 92.5mm, which can be reduced if desired by means of  $\frac{1}{4}$ "-40 brass tuning stubs located on the cavity (1).

The central discharge chamber for the plasma was fabricated from quartz tubing, 5mm o.d., 3mm i.d., and was approximately 3.5cm long. This chamber fit snugly into a quartz sleeve, 7mm o.d., 5mm i.d., which was left in the cavity at all times. This sleeve prevented introduction of any foreign material into the cavity while the chamber was replaced or adjusted during the initial setup procedures. Presumably, the quartz

sleeve would not be required for a plasma system of fixed configuration. A T-shaped chamber extended from the end of the plasma tube (Figure 2) and housed the modified microarc atomizer. The "T" was bent out of the optical path so thermal emission from the microarc was not seen by the detection system.

The microarc atomizer has been described previously (4) but was modified in this work to allow its stable and efficient operation in a helium environment. The operating voltage was increased from 900V, normally used with an argon microarc discharge, to 1800V to impart higher energy to the lower mass helium atoms. Also, the anode was made of thoriated tungsten (2% Th, Alfa Division, Ventron Corp., Danvers, Mass.) instead of stainless steel; the thoriated tungsten served to stabilize the discharge sooner after initiation. Conveniently, helium provides more rapid and more even heating of the tungsten sample filament than does argon. The filament was V-shaped and constructed of 0.5mm W wire; it would hold up to 10  $\mu$ l of sample solution.

The helium support gas for the microarc and plasma was supplied through a 16 gauge stainless steel syringe needle placed parallel to but above the microarc anode, with the tip of the needle back 5mm from the flat end of the thoriated tungsten anode. The range of flow rates of helium for stable microarc operation, efficient sample transport, and optimum plasma operation was experimentally determined to be between 300 and 450 ml/min. A flow rate of 400 ml/min optimized the time for sample transport through the plasma and provided greatest signal levels.

Figure 3 is a schematic diagram of the instrumental array. The power supply was a continuously variable, 100W microwave generator (Model HV-15A,

Scintillonics, Inc., Fort Collins, Colo.) operating at 2450 MHz. A coaxial cable, type RG/8, (Belden Corp., Richmond, Indiana) transmitted the microwave power to a double-stub tuner (Model 306A, PRD Electronics, Westbury, L.I., N.Y.) which was connected to the UG/58 RF connector (#82-24, Amphenol, RF Division, Danbury, Conn.) located on the cavity. High-purity helium (99.999%) was used for the microarc and microwave plasma. The microarc power supply has been described previously (4). A plano-convex lens, of aperture  $f/4$ , gathered the output radiation from the plasma and focussed it on the entrance slit of a medium resolution monochromator (Model EU-70C, Heath Co., Benton Harbor, Mich.). A Hamamatsu R212 photomultiplier tube (HTV Co., Ltd., Middlesex, N.J.) was used. A picoammeter (Model 427, Keithley Instruments, Inc., Cleveland, Ohio) converted the phototube current to a voltage which was output to either a chart recorder (Model SR-204, Heath Schlumberger Instruments, Benton Harbor, Mich.) for recording peak height information or a PDP-12 laboratory minicomputer (Digital Equipment Corp., Maynard, Mass.). The minicomputer was programmed in FORTRAN IV to calculate the peak area of the output signal, but was not used for control of any part of the experimental system.



DISCUSSION

Ignition of the Plasma When borosilicate glass tubing is used as the plasma chamber material, the helium plasma is self-igniting at atmospheric pressure, when the reflected power is tuned below 10W. Presumably, self-ignition occurs because of microwave heating of the glass, which then releases enough charged species to couple with the intense microwave field. The gaseous species act to supply electrons to "seed" the helium and lead to plasma ignition. No attempt was made in this work to identify these "seed" species, since the borosilicate glass was deemed unsuitable for use as a plasma tube material because of its short usable lifetime.

When quartz tubing was employed for the plasma chamber, an insufficient amount of ionizable material was volatilized to enable the plasma to self-ignite. However, it was found possible to ignite the plasma by striking the helium microarc. Enough material is ordinarily ejected from the white-hot microarc cathode filament to "seed" the helium and lead to ignition. Nonetheless, to enhance reliability, routine determinations were performed using a Tesla coil to initiate the helium plasma.

Tuning of the Cavity Insertion of the quartz plasma chamber into the cavity did not markedly affect the tunability of the cavity. Tuning could be accomplished with either the brass tuning screws on the cavity or with the double-stub tuner on the UG/58 RF connector. Either method produced the same results; consequently, the cavity was regularly tuned using the double-stub tuner, so the holes for the on-cavity tuning screws could be employed for cooling (see below).

The plasma ignited readily whenever the reflected power was tuned

below 20W and 75W were directed to the cavity. Once the plasma was ignited, the reflected power could be easily tuned to 0W.

Power Applied The microwave power supply was generally run at 100W forward power (FP). Exact measurements of the microwave power dissipated in the plasma were not taken, although the power utilized by the plasma was clearly less than the 100W applied since some of this power was lost as heat by the cavity.

Cooling The cavity thermally stabilized after approximately 15 minutes from the time of first plasma ignition. The external skin temperature of the cavity was about 90°C with 100W FP applied.

The utility of cooling the cavity was investigated. Using the double-stub tuner for tuning, the on-cavity tuning screws were removed and the holes used for cooling of the cavity, with the hole on the outer edge of the cavity being used as the cooling gas inlet. The cooling gas was passed through a drying trap and a cooling coil (in liquid N<sub>2</sub>) before entering the cavity. Plasma operation and signal-to-noise ratio were not significantly affected by cooling with air, nitrogen, argon, or helium, and so no cavity cooling was used.

Plasma Stability The stability of the plasma was determined by monitoring the 471.3nm He I line. The time constant of the detection system was 0.3 sec. Fluctuation of the emission from this line was less than 1% over 3 hours, after a warm-up period of approximately 15 minutes.

Plasma Positioning The plasma exists as a filament approximately 8-10mm long and 1mm in diameter in the center of the 3mm i.d. chamber. The helium plasma never extended past the internal cavity walls, at any flow

rate, whereas the Argon plasmas usually extend about 5mm out the ends of the cavity. With 50W FP or less, the plasma always existed exactly in the center of the chamber; intensity of emitted radiation was greatest at the plasma center and decreased smoothly out to the chamber walls. Above 50W FP the plasma would rest along the inner wall of the chamber. The plasma never moved position once it ignited along the wall, resulting in etching of the quartz wall over a period of time. This etched region served as a site for collection of analyte vapor and led to undesired analyte memory effects and broadened signal peaks. Consequently, the chamber must be replaced after about 40 hours of plasma operation, if plasma powers over 50W are employed.

Background Characteristics MIPs generally exhibit uncomplicated background spectra. However, a wavelength scan (200-600nm) of the background from the present atmospheric-pressure helium plasma showed a significant number of prominent spectral features of both line and broadband character. The wavelength location and relative intensities of the majority of these features were recorded and compared to those of molecular species expected in such a plasma (6,7). Table I is a compilation of the strongest features found and indicates the species causing each feature. The presence of all of the identified molecular bands and lines can be understood with the aid of the excitation mechanisms for this plasma postulated by Beenakker (3). Because most of the observed molecular features originated from excitation of atmospheric species, it was possible to reduce their level simply by closing off the viewing end of the plasma chamber with a quartz window. It also would be possible to eliminate many of these features using wavelength modulated detection (8).

Plasma Temperature A non-rigorous determination of the excitation temperature of the plasma was made for comparative purposes with similar MIPs. The relative intensities of He I lines, shown in Table II, were measured and a plot of  $\log [I\lambda / g_k A_{1k}]$  v.s.  $E_k$  was made (9,10). The slope of this plot yielded an excitation temperature of  $7250^\circ\text{K}$  for this plasma. This temperature compares well with other argon and helium MIPs whose excitation temperatures vary between  $4500$  and  $8300^\circ\text{K}$  (11).

Nebulization It was verified that the new helium MIP can operate continuously during input of a nebulized aerosol, as claimed by Beenakker (1). However, the plasma is obviously weakened by the injected aerosol (about  $0.1$  ml/min maximum) and becomes less stable. Nonetheless, the resistance of the plasma to extinction by an aqueous aerosol indicates its durability, compared to others which have been reported. (4, 11)

Analytical Calibration Curves Figure 4 shows analytical calibration curves for Zn I ( $213.8\text{nm}$ ), Pb I ( $216.9\text{nm}$ ), Mn I ( $279.5\text{nm}$ ,  $403.1\text{nm}$ ), Mg I ( $285.2\text{nm}$ ) and Cu I ( $324.7\text{nm}$ ). The plots are linear and, in most cases, have a slope of 1.0. Dynamic ranges vary from 2 to 5 orders of magnitude. Both Mn ( $279.5\text{nm}$ ) and Mg ( $285.2\text{nm}$ ) were affected by instability in the strong OH spectral background features which overlap these lines, causing a decrease in dynamic range and worsening in detection limit for both elements.

Figure 5 shows analytical calibration curves for easily ionized elements, specifically, Ca II ( $393.4\text{nm}$ ), Ca I ( $422.7\text{nm}$ ), and Na ( $589.0\text{nm}$ ). The curve for Ca I ( $422.7\text{nm}$ ) is typical of many elements; the upper end of the dynamic range is limited presumably by the excitation of calcium atoms to higher excited states, necessitating the use of other lines. It was expected the Ca would be appreciably ionized in this plasma, and so one Ca II line was

examined. The curve for the Ca II (393.4nm) line is reasonably linear and has a slope of 1.08. Clearly the high excitation capability of this plasma would necessitate the examination of a number of Ca lines for the optimum SNR and dynamic range for an analysis to be realized.

It was necessary to add 100  $\mu\text{g}/\text{ml}$  Rb to each Na standard solution to obtain data for the Na (589.0nm) analytical curve. The bending-off of the curve is assumed to be caused by self-absorption by atoms exiting at the cooler viewing end of the chamber.

Detection Limits Table III compares detection limits obtained for a number of elements using the new helium MIP with those cited in recent publications (11, 12). The new MIP detection limits compare well with those obtained with both single-shot and continuous nebulization sample injection MIP systems. Significantly, the detection limits obtained on the present single-shot He MIP system were calculated on the basis of the  $1\mu\text{l}$  sample aliquot actually used, and therefore represent routinely obtainable values.

Interferences MIPs have been noted to be affected by the introduction of relatively large amounts of sample material ( $\sim 1\mu\text{g}$  absolute). However, the new plasma remained ignited during injection of sample material up to the maximum amount atomizable from the microarc used, about  $5\mu\text{g}$  absolute. Of course, the relative standard deviation of the measured signal degrades as larger and larger amounts of material are atomized into the plasma; however, the plasma remains ignited and, in that sense, proves to be a significantly more durable source than many previous MIPs.

As suggested earlier, ionization interferences are expected in any MIP, and in the new plasma a significant amount of ionization of any easily

ionizable element (e.g. Ca, Na, Li) appears to occur. As in most determinations, an ionization suppressant can be employed to overcome such interferences. Further examination of ion emission lines is warranted to determine their analytical utility.

Refractory elements, such as Al and Si, have been found to exert little effect on analyte signals in the plasma. This result is not unexpected in view of the use of the microarc sample atomizer (4). However, further investigations of solute vaporization interferences are necessary and are currently underway.

CONCLUSIONS

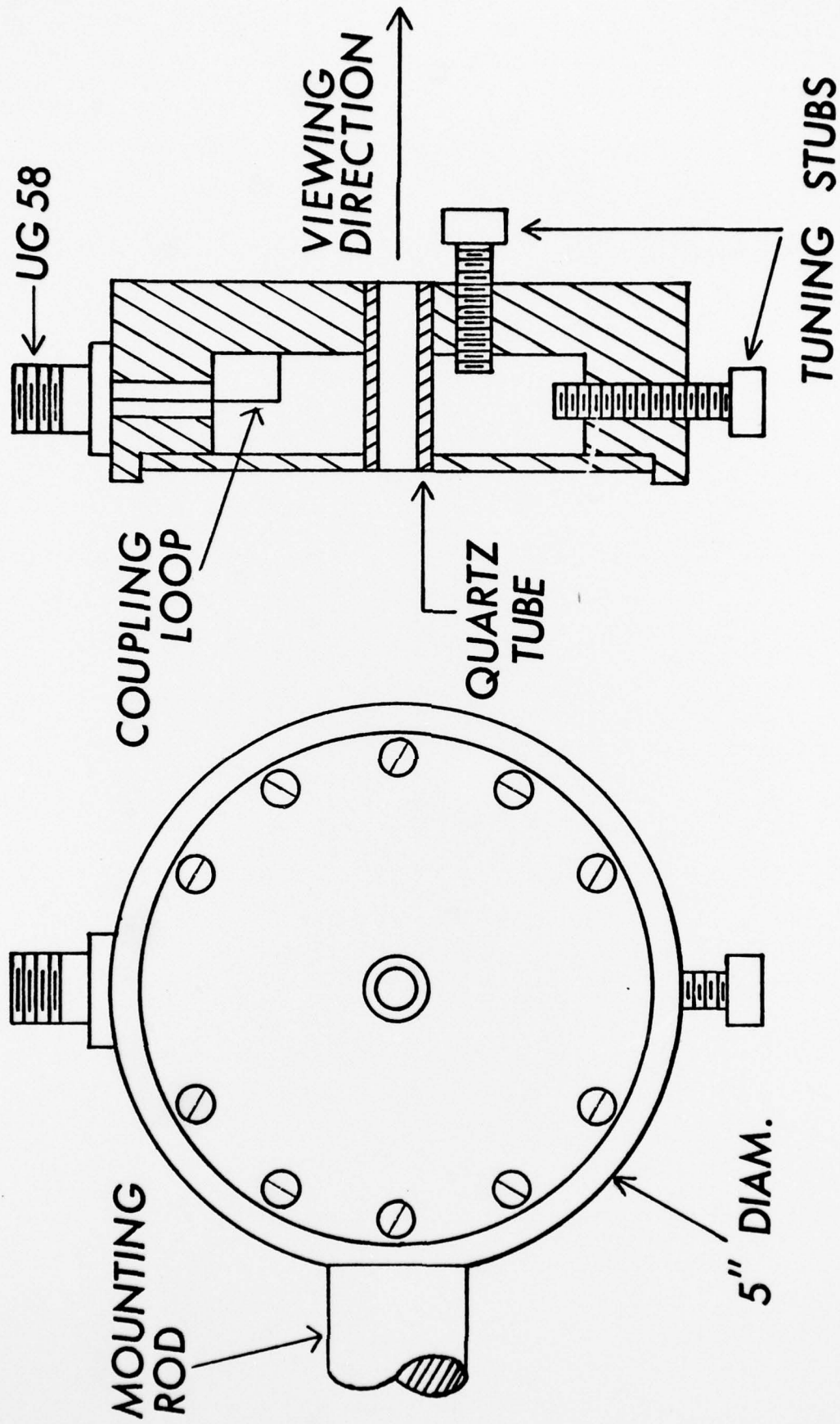
The atmospheric pressure, helium microwave-induced plasma generated in the cavity designed by Beenakker (1) is a durable, stable, and highly efficient excitation source for emission spectrometry of metallic elements. It is easy to ignite and operate and uses low volumes of inert support gas. Moreover, the cavity does not require cooling. Although injected material does lead to reduced excitation efficiency and increased instability, this MIP exhibits a significant improvement over other versions of microwave-induced plasma in its tolerance of sample and solvent material. The high temperature of the new plasma leads to increased ionization and population of higher excited states; this result requires careful choice of emission lines to be used for analytical measurement. Dynamic background correction should prove useful with this plasma for the elimination of broadband molecular emissions.

- 1 C.I.M. Beenakker, *Spectrochim. Acta*, 31B, 483 (1976).
- 2 C.I.M. Beenakker, Paper #305, Pittsburgh Conference on Analytical Chemistry and Applied Spectroscopy, Cleveland, Ohio, March, 1977.
- 3 C.I.M. Beenakker, *Spectrochim. Acta*, 32B, 173 (1977).
- 4 L.R. Layman, G.M. Hieftje, *Anal. Chem.*, 47, 194 (1975).
- 5 S. Ramo, J. R. Whinnery, Fields and Waves in Modern Radio, 2nd Edition, John Wiley & Sons, Inc., New York, 1953.
- 6 A. G. Gaydon, The Spectroscopy of Flames, 2nd Edition, John Wiley & Sons, Inc., New York, 1974.
- 7 I. Kopp, R. Lindgren, B. Rydh, Table of Band Features of Diatomic Molecules by Wavelength Order, Version A, Inst. of Physics, University of Stockholm.
- 8 P.M. Houpt, *Anal. Chim. Acta*, 86, 129 (1976).
- 9 K. Fallgatter, V. Svoboda, J. D. Winefordner, *Appl. Spec.*, 25, 347 (1971).
- 10 W.L. Wiese, M.W. Smith, B.M. Glennon, Atomic Transition Probabilities-Hydrogen Through Neon, NSRDS-National Bureau of Standards, 4, Vol. 1 (U.S. Govt. Printing Office, Washington, D.C.) 1966.
- 11 R.K. Skogerboe, G.N. Coleman, *Anal. Chem.*, 48, 611A (1976).
- 12 S. Greenfield, H. McD. McGeachin, P.B. Smith, *Talanta*, 22, 553 (1975).

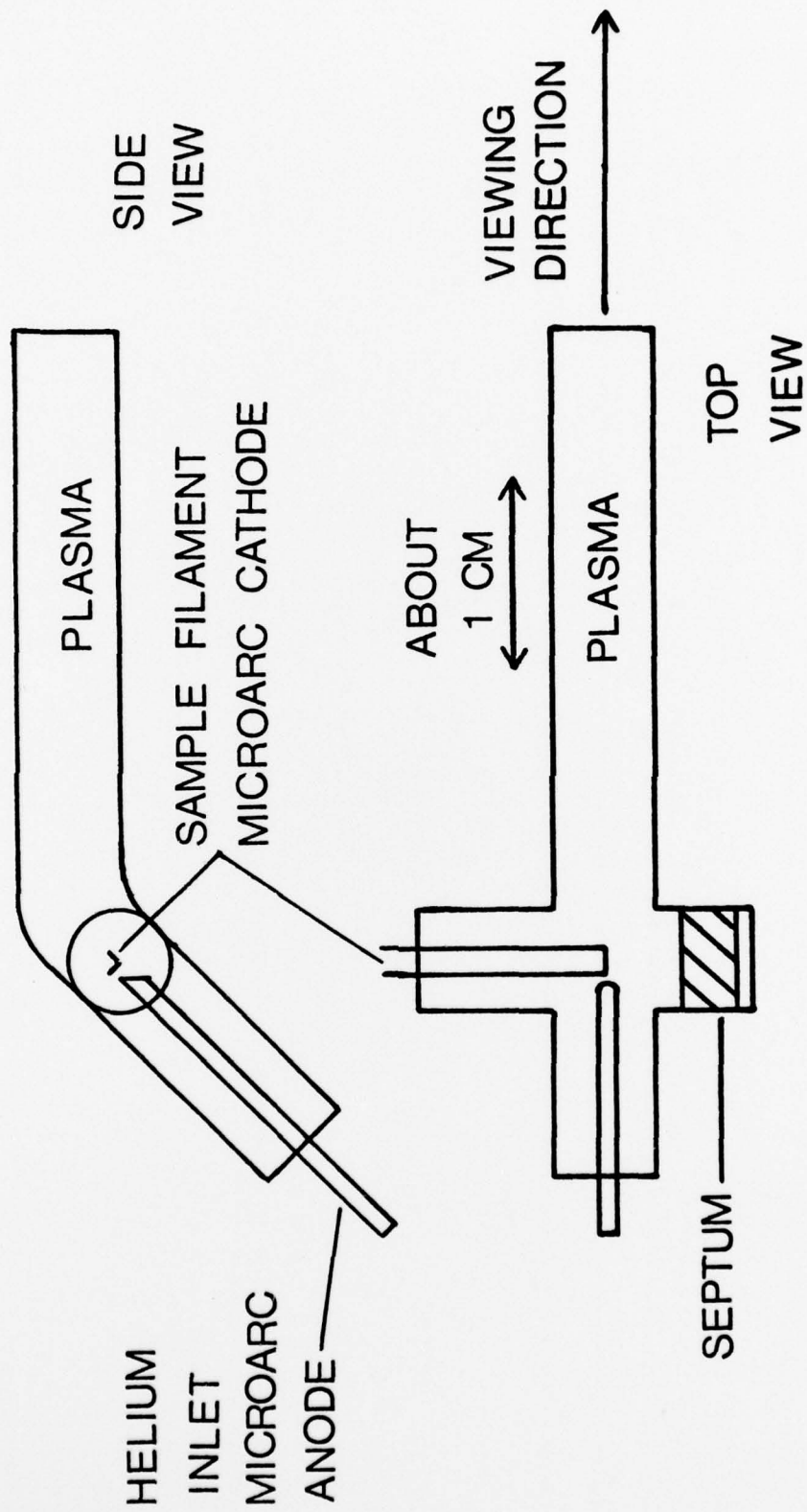


FIGURE CAPTIONS

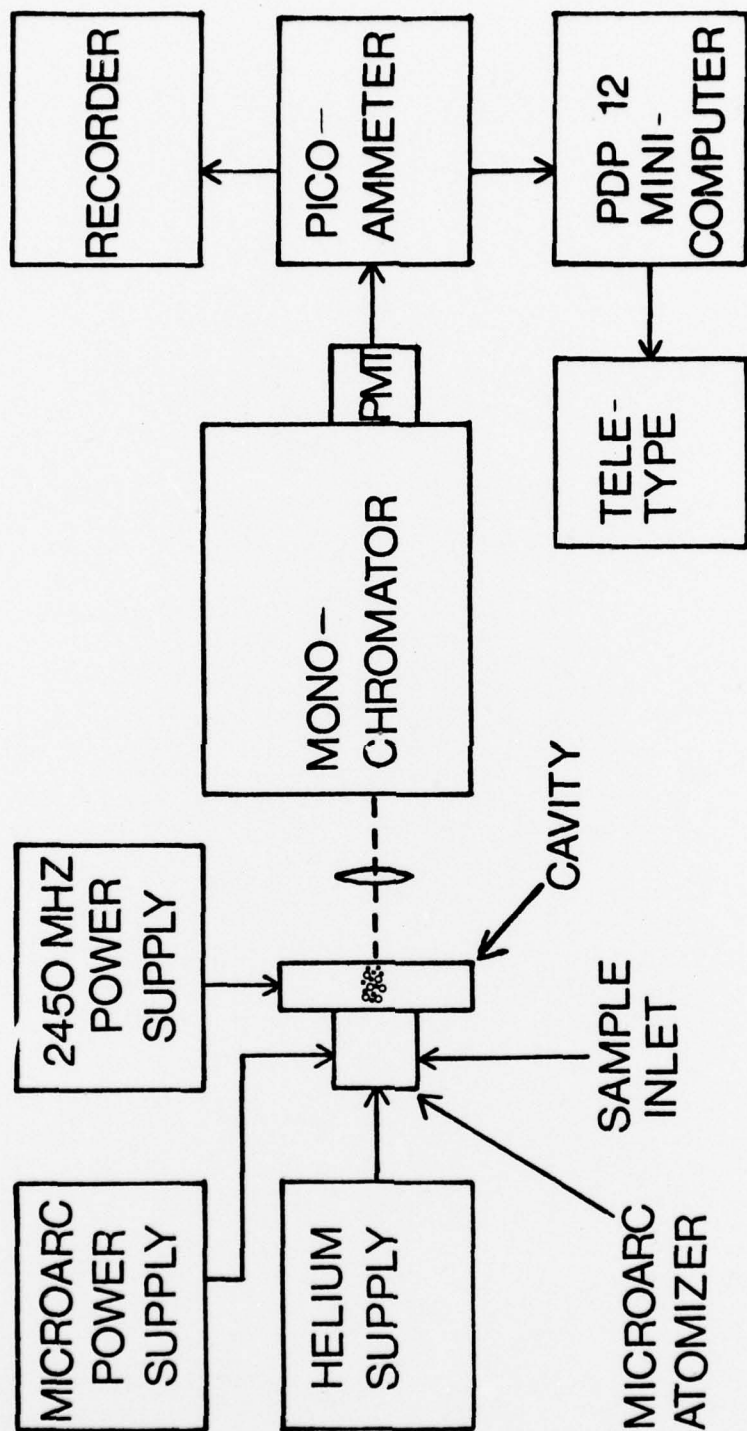
1. Diagram of 2450 MHz Microwave Resonant Cavity. Inside cavity diameter=9.25cm. Cavity material-copper (hatched area). Quartz sleeve=7mm o.d., 5mm i.d.
2. Diagram of Quartz Plasma Chamber. Tubing is 3mm i.d., 5mm o.d. and fits inside quartz sleeve of Figure 1.
3. Schematic Diagram of Instrumental Array
4. Analytical Calibration Curves for:
  - a. Zn I (213.8nm)
  - b. Pb I (216.9nm)
  - c. Mn I (279.5nm)
  - d. Cu I (324.7nm)
  - e. Mg I (285.2nm)
  - f. Mn I (403.1nm)
5. Analytical Calibration Curves for:
  - a. Na I (589.0nm)
  - b. Ca II(393.4nm)
  - c. Ca I (422.7nm)

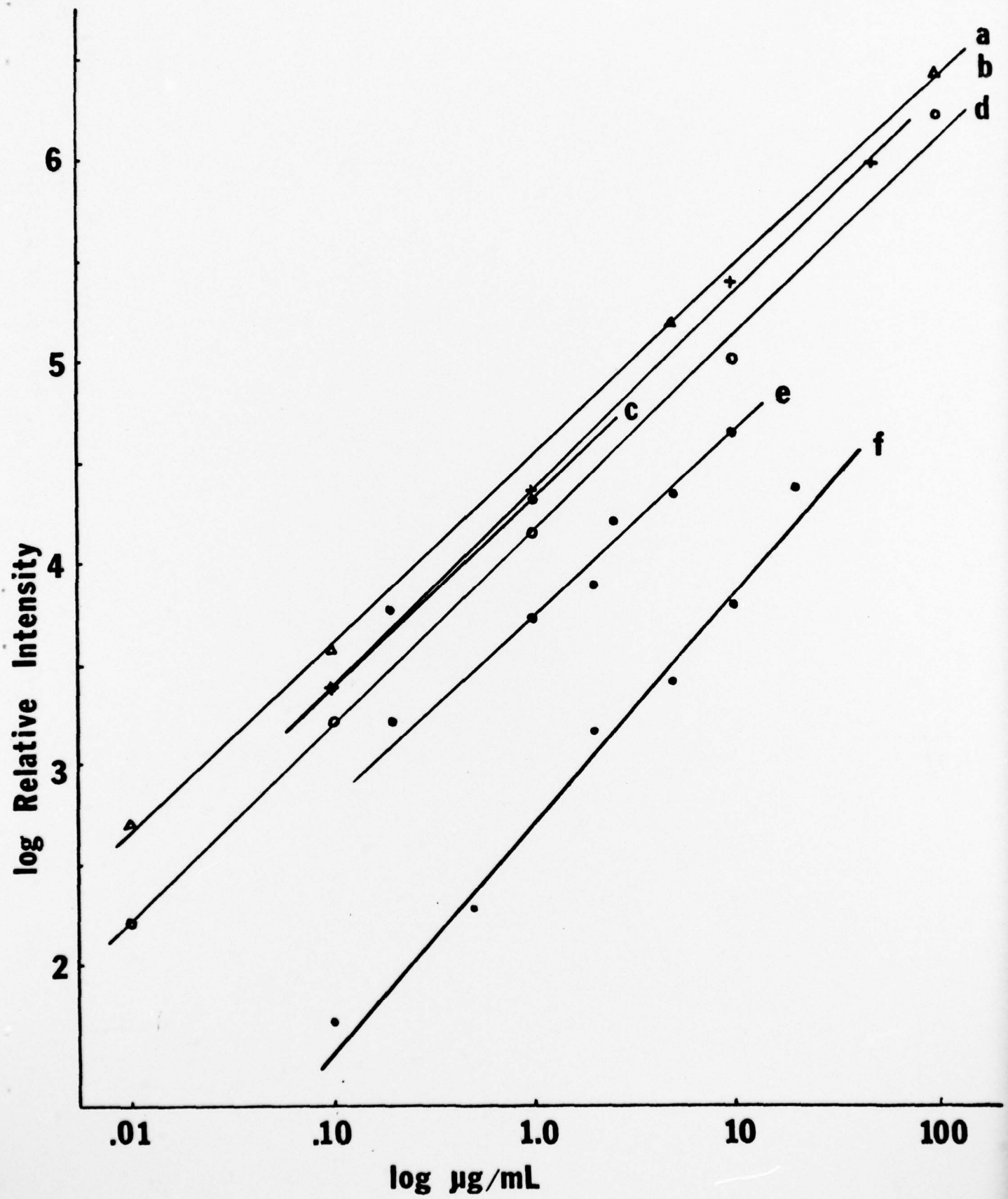


2450MHZ RESONANT CAVITY



QUARTZ PLASMA CHAMBER





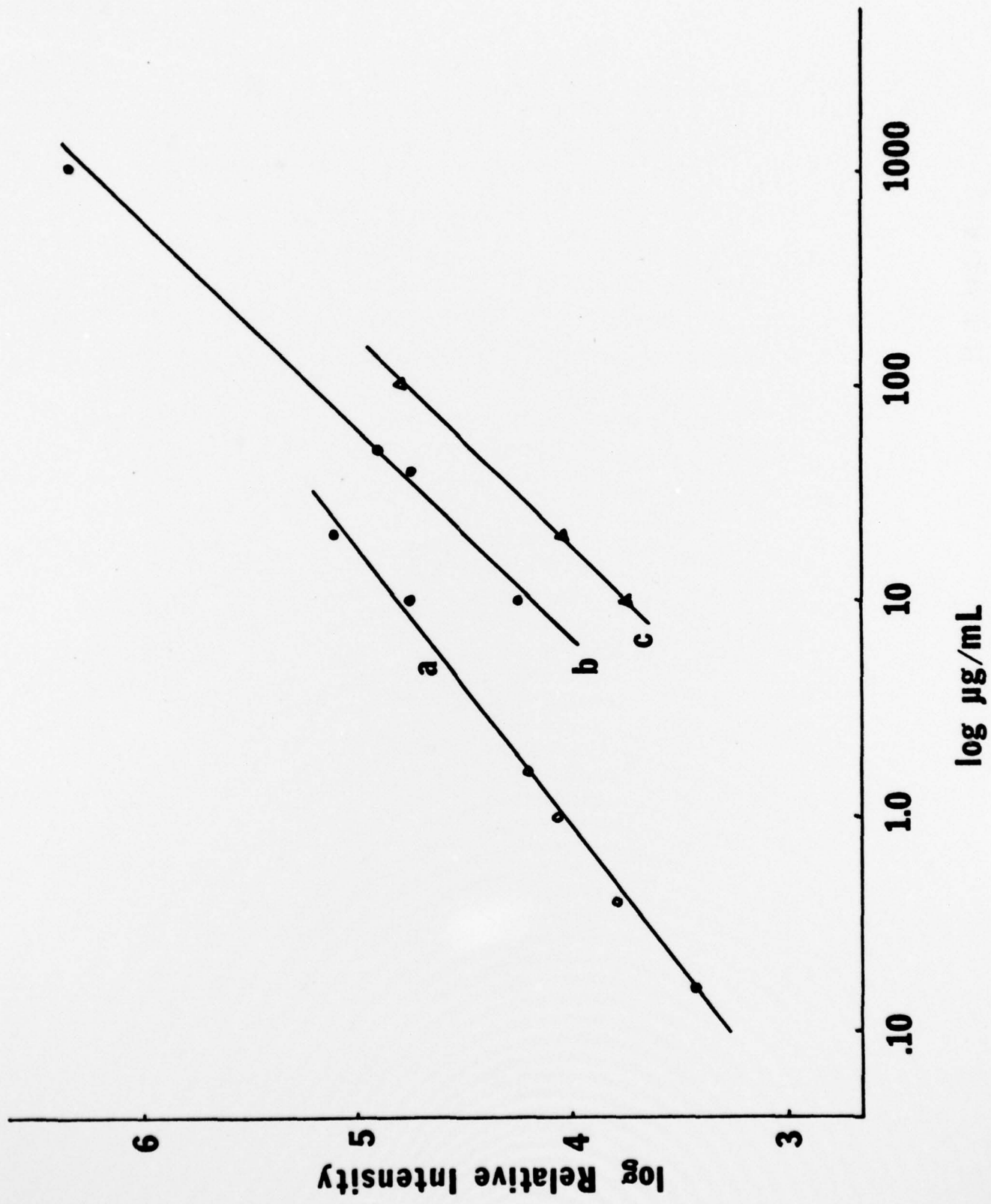


TABLE I Most Prominent Background Spectral Features in the Atmospheric-Pressure Helium MIP

| <u>Originating Species</u> | <u>Wavelength(nm)</u> | <u>Transition</u>          |
|----------------------------|-----------------------|----------------------------|
| NO                         |                       | $[A^2 \Sigma^+ - x^3 \Pi]$ |
|                            | 205.24                | (2,0)                      |
|                            | 215.49                | (1,0)                      |
|                            | 226.94                | (0,0)                      |
|                            | 237.02                | (0,1)                      |
|                            | 247.87                | (0,2)                      |
|                            | 259.57                | (0,3)                      |
| OH                         |                       | $[^2 \Sigma^+ - ^2 \Pi]$   |
|                            | 281.13                | (1,0)                      |
|                            | 287.53                | (2,1)                      |
|                            | 294.52                | (3,2)                      |
|                            | 306.36                | (0,0)                      |
| NH                         |                       | $[A^3 \Pi - x^3 \Sigma^-]$ |
|                            | 336.00                | (0,0)                      |
|                            | 337.09                | (1,1)                      |
| N <sub>2</sub>             |                       | $[^3 P_u - B^3 P_g]$       |
|                            | 357.69                | (0,1)                      |
|                            | 375.54                | (1,3)                      |
|                            | 380.49                | (0,2)                      |

TABLE II He I Emission Line Data Used for Calculating Excitation Temperatures

| $\lambda$ (nm) | $E_k$ ( $\text{cm}^{-1}$ ) | $g_k$ | $A_{1k}$ ( $\times 10^{-8} \text{ sec}^{-1}$ ) <sup>a</sup> |
|----------------|----------------------------|-------|-------------------------------------------------------------|
| 388.8          | 185 565                    | 9     | .09478                                                      |
| 501.5          | 186 210                    | 3     | .1338                                                       |
| 471.3          | 190 298                    | 3     | .106                                                        |
| 504.7          | 190 940                    | 1     | .0665                                                       |
| 447.1          | 191 445                    | 15    | .251                                                        |
| 492.1          | 191 447                    | 5     | .202                                                        |
| 396.4          | 191 493                    | 3     | .0717                                                       |
| 412.0          | 193 347                    | 3     | .430                                                        |
| 443.7          | 193 663                    | 1     | .0313                                                       |
| 402.6          | 193 917                    | 15    | .117                                                        |
| 438.7          | 193 918                    | 5     | .0907                                                       |
| 416.8          | 195 115                    | 1     | .0176                                                       |
| 381.9          | 195 260                    | 15    | .0589                                                       |
| 383.3          | 197 213                    | 5     | .00971                                                      |

a. From ref. 10.



TABLE III Detection Limits Obtained with the New MIP (pg)

| <u>Element</u>  | <u>Wavelength (nm)</u> | <sup>a</sup> <u>He MIP</u> | <sup>b</sup> <u>Ar MIP</u> | <sup>c</sup> <u>Other Systems</u> |
|-----------------|------------------------|----------------------------|----------------------------|-----------------------------------|
| An              | 213.8                  | 0.35                       | 9.2                        | 1.0-6.0                           |
| Pb              | 216.9                  | 0.56                       | 3.8                        | 50                                |
| Mu              | 279.5                  | 0.46                       | -                          | -                                 |
|                 | 403.1                  | 20                         | -                          | 5.40                              |
| Mg              | 285.2                  | 0.85                       | 0.45                       | 50                                |
| Cu              | 324.7                  | 0.42                       | 1.6                        | 5.0                               |
| Ca              | 422.7                  | 1.6                        | 10                         | 50                                |
| Ca <sup>+</sup> | 393.4                  | 1100                       | -                          | -                                 |
| Na              | 589.0                  | 0.12                       | 0.01                       | 10                                |

a. 1 $\mu$ l sample aliquot

b. 10 $\mu$ l sample aliquot,  $\mu$ -arc Atomizer. Taken from ref. 4.

c. calculated for 10  $\mu$ l sample aliquot. Taken from refs. 11 and 12.

#### ACKNOWLEDGEMENT

The authors would like to thank C.I.M. Beenakker for useful discussions concerning the use of his new cavity. Also, we greatly appreciated the assistance of Rodney K. Williams in early stages of the investigation.

#### CREDIT

Supported in part by the Office of Naval Research, by the National Institutes of Health through grant PHS GM 17904-05, and by the National Science Foundation through grant CHE 76-10896.

TECHNICAL REPORT DISTRIBUTION LIST

| <u>No. Copies</u> |                                                                                                                              | <u>No. Copies</u>                                                                                                    |
|-------------------|------------------------------------------------------------------------------------------------------------------------------|----------------------------------------------------------------------------------------------------------------------|
| 2                 | Office of Naval Research<br>Arlington, Virginia 22217<br>Attn: Code 472                                                      | Defense Documentation Center<br>Building 5, Cameron Station<br>Alexandria, Virginia 22314 12                         |
| 6                 | Office of Naval Research<br>Arlington, Virginia 22217<br>Attn: Code 102IP 1                                                  | U.S. Army Research Office<br>P.O. Box 12211<br>Research Triangle Park, N.C. 27709<br>Attn: CRD-AA-IP 1               |
| 1                 | ONR Branch Office<br>536 S. Clark Street<br>Chicago, Illinois 60605<br>Attn: Dr. Jerry Smith                                 | Naval Ocean Systems Center<br>San Diego, California 92152<br>Attn: Mr. Joe McCartney 1                               |
| 1                 | ONR Branch Office<br>715 Broadway<br>New York, New York 10003<br>Attn: Scientific Dept.                                      | Naval Weapons Center<br>China Lake, California 93555<br>Attn: Head, Chemistry Division 1                             |
| 1                 | ONR Branch Office<br>1030 East Green Street<br>Pasadena, California 91106<br>Attn: Dr. R. J. Marcus                          | Naval Civil Engineering Laboratory<br>Port Hueneme, California 93041<br>Attn: Mr. W. S. Haynes 1                     |
| 1                 | ONR Branch Office<br>760 Market Street, Rm. 447<br>San Francisco, California 94102<br>Attn: Dr. P. A. Miller                 | Professor O. Heinz<br>Department of Physics & Chemistry<br>Naval Postgraduate School<br>Monterey, California 93940 1 |
| 1                 | ONR Branch Office<br>495 Summer Street<br>Boston, Massachusetts 02210<br>Attn: Dr. L. H. Peebles                             | Dr. A. L. Slafkosky<br>Scientific Advisor<br>Commandant of the Marine Corps (Code RD-1)<br>Washington, D.C. 20380 1  |
| 1                 | Director, Naval Research Laboratory<br>Washington, D.C. 20390<br>Attn: Code 6100                                             | Office of Naval Research<br>Arlington, Virginia 22217<br>Attn: Dr. Richard S. Miller 1                               |
| 1                 | The Asst. Secretary of the Navy (R&D)<br>Department of the Navy<br>Room 4E736, Pentagon<br>Washington, D.C. 20350            |                                                                                                                      |
| 1                 | Commander, Naval Air Systems Command<br>Department of the Navy<br>Washington, D.C. 20360<br>Attn: Code 310C (H. Rosenwasser) |                                                                                                                      |